national accelerator laboratory

TM-472
2200.

500 GeV NEUTRINO BEAM AT NAL

D. C. Carey, L. J. Edwards, Y. W. Kang,

F. A. Nezrick, R. J. Stefanski and T. E. Toohig

October 1970

Abstract

The parameters of 500 GeV neutrino beam have been determined as follows:

Decay length = 400 meters

Decay tunnel diameter = 36"

Shield length = 1000 meters

Distance between the end of the shield and the bubble chamber = 25 meters

The length of the target box = 200'

On the basis of the above parameters the neutrino energy distributions are given for 500 GeV and 200 GeV, respectively.

INTRODUCTION

The neutrino beam in the Neutrino Laboratory at NAL has evolved under the anticipation of new particle physics, technological breakthroughs in the Accelerator construction, and economical restraints. The beam design started with a rather conventional concept of low energy neutrino physics. It has been modified rapidly by a possibility of the initial operation of 500 GeV Accelerator and realization of the extreme importance of high energy neutrino interactions ($\gtrsim$100 GeV) in current particle physics.

The 500 GeV neutrino beam facility consists of a 400 m long decay tunnel and a 1000 m long soil shield, and is followed by the Neutrino Laboratory B and the Neutrino Laboratory C. A removable hadron beam dump is located at the end of the decay tunnel, where a muon beam and a hadron beam initiate.

The facility is characterized by a pure soil shield. This is due to the difficulties encountered in muon groundshine suppression around the bubble chamber area even after a modest investment of iron shield. A combination of iron and soil also does not provide efficient shielding due to the multiple Coulomb scattering. Despite its length, the present beam will provide a reasonable number of neutrino events in the 15-foot bubble chamber, insuring an efficient operation of the chamber.

The construction of the neutrino beam facility in the neutrino laboratory is likely to proceed more rapidly than the development of sophisticated focusing devices for the beam. Indeed it is likely that some of the initial operation of the beam will be conducted without a focusing device or with a simple quadrupole triplet focusing system. Although operation under these conditions has some disadvantages -- such as a low neutrino flux and a possibly high antineutrino background -- much useful research can be carried out in this kind of beam. In particular, studies can be undertaken to determine the effectiveness of the muon shield and various monitoring systems, to study the difficulties involved in operating the decay tunnel in vacuum or in air, and to develop techniques required to operate magnets in the target box. The initial development and testing of the experimental detectors, and also the initial experiments themselves, could be carried out in this beam. In this regard, this paper presents estimates of neutrino flux for the NAL neutrino beam under a variety of focusing conditions, but in particular, for the conditions anticipated for the initial operation of the beam.

PARAMETERS FOR THE CALCULATIONS

The computation of the neutrino flux is carried out with the computer program NUADA[1]. The program requires as input data a particle yield spectrum and the geometric parameters of the beam and focusing devices. The input spectrum is divided into bins of production angle and momentum; a ray from the center of each bin is traced through the focusing device and along the beam; the ray is allowed to decay to neutrinos at regular intervals along its path; the contribution to the neutrino flux is determined at each decay point; and the final neutrino flux is weighted according to the yield spectrum.

As an input yield spectrum for the program, the CKP formula is used[2] because of its simple closed form. The CKP formula and the specific parameters used, are given in the Appendix. Because of the large variations that exist in the predictions of various production models, it is useful to give some comparisons and therefore results from the Hagedorn-Ranft predictions will be given[3]

The geometric parameters of the neutrino beam have now been fixed in preparation for the Title I report for the area. These parameters, which were also used in the computations, are summarized in Table I.

DEFINITION OF ZERO AND PERFECT FOCUSING

It is useful to compare the neutrino flux calculations for any focusing device with the flux obtained under perfect focusing and zero focusing conditions. In the perfect focusing calculation, each ray is placed on the beam axis as soon as it leaves the target. This then yields the maximum obtainable neutrino flux under the physical conditions of the beam. The zero focusing calculation gives the neutrino flux when no focusing device is present. The comparison of the ν-flux obtainable with a focusing device with the perfect and zero focus spectra then gives a measure of the effectiveness of the focusing system.

In the calculations the target was assumed a line source: The target thickness was used only to estimate the attenuation of secondaries as they escape the target. This simplification is necessary to make the calculations tenable; i.e., to reduce the computer time required for the calculations. This assumption does not affect the perfect focusing results, and has little affect on the zero focus and single quadrupole triplet focus spectra. For the more sophisticated devices this assumption might lead to an overestimate of the neutrino flux.

NEUTRINO FLUX FOR A SINGLE QUADRUPOLE TRIPLET FOCUS

To enhance the neutrino flux during the initial running of the neutrino beam, a single quadrupole triplet would be used.[4] To expedite matters, only main ring quadrupoles would be considered. The properties of these quadrupoles is summarized in Table II. In the neutrino flux calculations, particles were assumed to enter the quadrupole in a plane rotated forty-five degrees from the horizontal plane. The aperture was assumed to be a 2-inch radius in this plane. Under normal conditions the usable main ring quadrupole aperture is 2-inches vertical by 5-inches horizontal. However, the restrictions in field gradient for a quadrupole focused ν-beam are far less severe than in normal beam design making the effective aperture larger in our calculations. The aperture of the quadrupole[5,6] is shown in Figure 1. The geometry of the quadrupole aperture is important to the calculation of ν-flux only at the lowest parent energies being focused.

The length of the quadrupole triplet is dependent on the incident beam energy.[7] At lower energies, greater solid angle acceptance is required and the triplet must be shorter. The two cases of 500 GeV and 200 GeV operation were considered. The arrangement of the quadrupoles in the target box is given in

Figure 2 for these two cases. Slits are used to protect the front quads from low energy radiation from the target. DC power consumption for the 500 and 200 GeV channels is 680 and 420 kW respectively.

The results for the 500 GeV calculation are given in Figure 3a-c. Figure 3a gives the neutrino flux at the maximum current setting. In this configuration, the quadrupoles serve to reduce the low-energy contamination while giving some enhancement to the high energy flux. At an intermediate current setting, as in Figure 3b, the quadrupoles act as a broad band focusing device. Figure 3c gives a low current setting in which some slight enhancement is given to the low energy flux.

The results for the 200 GeV operation are given in Figure 4. Here we give only the current setting at which a broad band focusing is achieved. A variation in current changes the flux in a similar fashion to the 500 GeV case.

The characteristic double bump that occurs in the quadrupole flux curves is due to the difference in mass between kaons and pions. The quadrupole triplet will focus particles at the detector within some narrow momentum band. Because of the decay kinematics, pions will decay to neutrinos of lower energy than those from kaon decays. Thus, the bump at low energy arises from pion decays, while that at higher energies occurs because of kaon decays.

THE PULSED HORN SYSTEM

A pulsed horn system with a pulsed period up to 1 msec offers a highly efficient focusing capability to a neutrino beam. It has been shown at CERN and BNL that the system can operate steadily for a considerable time. The system is particularly advantageous for the broad band and an active development for a narrow band beam is being now pursued here.

It is interesting to note that a previously described horn[9] is still efficient for the present beam if we adjust the locations of the target and the second horn with respect to the first horn. The present calculations for real focusing were done with the old horn system arranged inside the target box.[10] However, a final shape of the horn system which would be installed in the future, might be quite different from this horn. At the present the flux for real focusing is about 50% of that for perfect focusing.

In Figure 5 and Figure 6 are given the neutrino fluxes for perfect, real, and no focusing for 500 GeV and 200 GeV operations, respectively. The ratio of fluxes for perfect to no focusing is 3 to 5 at high energy and about 10 in the peak region where the focusing advantage is quite prominent.

THE HAGEDORN-RANFT MODEL PREDICTION

The neutrino flux distributions obtained from the production spectrum of the Hagedorn-Ranft model are given in Figure 7 for perfect and no focusing cases, for 500 GeV and 200 GeV operations, respectively. Of particular interest is the enormous difference in predictions of this and the CKP model of the high energy flux while around 20 GeV the fluxes are roughly the same. Clearly the flux at high energy is in doubt by orders of magnitude. The cause of this discrepancy is two-fold. First, the high energy neutrinos are all the progeny of high energy kaons. The K to pi ratio of the Hagedorn-Ranft model is substantially higher than that used for CKP (0.33 as compared to 0.1 for CKP). Further, the shape of the Hagedorn-Ranft spectrum tends to favor the production of high energy secondaries.

APPENDIX

The CKP formula:

$$\frac{d^2N}{dEd\Omega} = \frac{n_\pi E^2}{2\pi P_c{}^2 T} \exp\left[-E\left(\frac{1}{T} + \frac{\theta}{P_c}\right)\right]$$

$n_\pi = 0.45\ E_o{}^{1/4} = 2.13$

$T = 0.3046\ E_o{}^{3/4} = 32.21$.

$P_c = 0.22$

E_o = Incident Proton Energy

E - Secondary Particle Energy

REFERENCES

[1]The program NUADA was originally developed at CERN under the name of NUFLUX and was modified for use at NAL by D.C.Carey.

[2]F.A.Nezrick, R.J.Stefanski, Y.W.Kang, D.C.Carey, Particle Production Spectra for Neutrino Beam Design, TM-196.

[3]M.Awschalom and T.O.White, Secondary Particle Production at 200 GeV, FN-191.

[4]A.Roberts, Simple High-Momentum Neutrino Beams, FN-124; D.C.Carey, Y.W.Kang, F.A.Nezrick, R.J.Stefanski and M.L. Stevenson, Quadrupole Long-Spill Neutrino Beams, TM-220.

[5]The lattice contour was taken from a note by E.Malamud and from prints made available by H.Barber of the Main Ring Section.

[6]We are grateful to S.Pruss and J.Schivell for field gradient measurements for main ring quadrupoles. Measurements in the horizontal plane indicate that the gradient varies by only a few percent out to 2" from the center of the magnet at 4000 amps.

[7]See also, L.C.Teng, Wide-Bank Quadrupole Focusing System for Neutrino and Muon Beams, FN-210.

[8]Taken from an Engineering Note by W.W.Nestander.

[9]Y.W.Kang and F.A.Nezrick, Neutrino Beam Design, 1969 Summer Study, (1960), SS-146.

[10]A target is located at 2.5 m and 3.5 m behind the first horn for 200 GeV and 500 GeV operations, respectively. The second horn is set at 60 m from the first horn for both operations but the better result is obtained for high energy neutrinos with the second horn at 100 m for 500 GeV operation.

TABLE I

BEAM PARAMETERS

Length of Target Box	200 ft. = 60 M
Length of Decay Tunnel	1333 ft. = 400 M
Length of Shield	3333 ft.= 1000 M
Recess between Detector and Shield	83 ft. = 25M
Decay Tunnel Radius	18 in. = 0.475 M
Detector Radius	(4.5 ft. = 1.35 M (Eff. Bubble Chamber Radius
Target Length	.03 Interaction length
Target radius	.079 in. - 2 mm

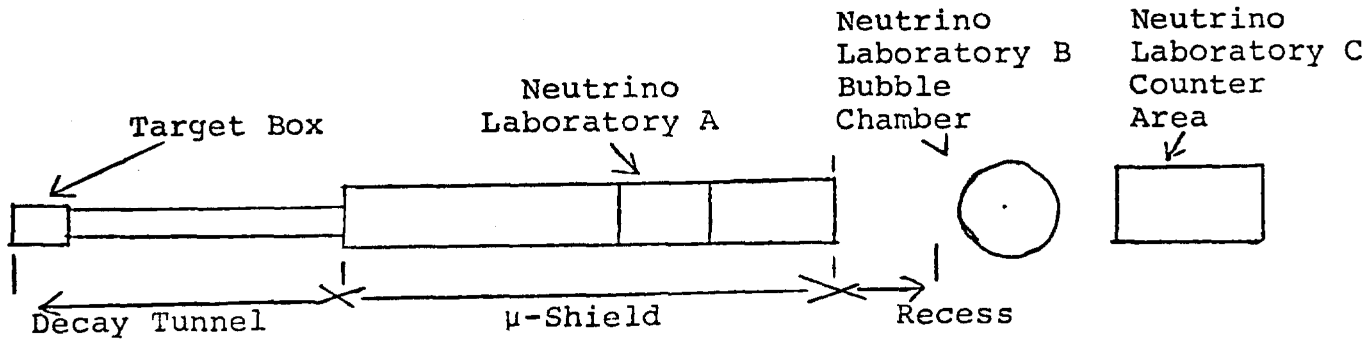

TABLE II

PROPERTIES OF MAIN RING QUADRUPOLES[8]

Maximum Current		4737 Amp
Field Gradient at Maximum Current		6.6 kG/in
Aperture		(See Figure 1)
Length		4.6 or 7.4 feet
Power	66.9	103.5 kW at maximum current
Temperature Rise	32.3	62.0° at maximum current

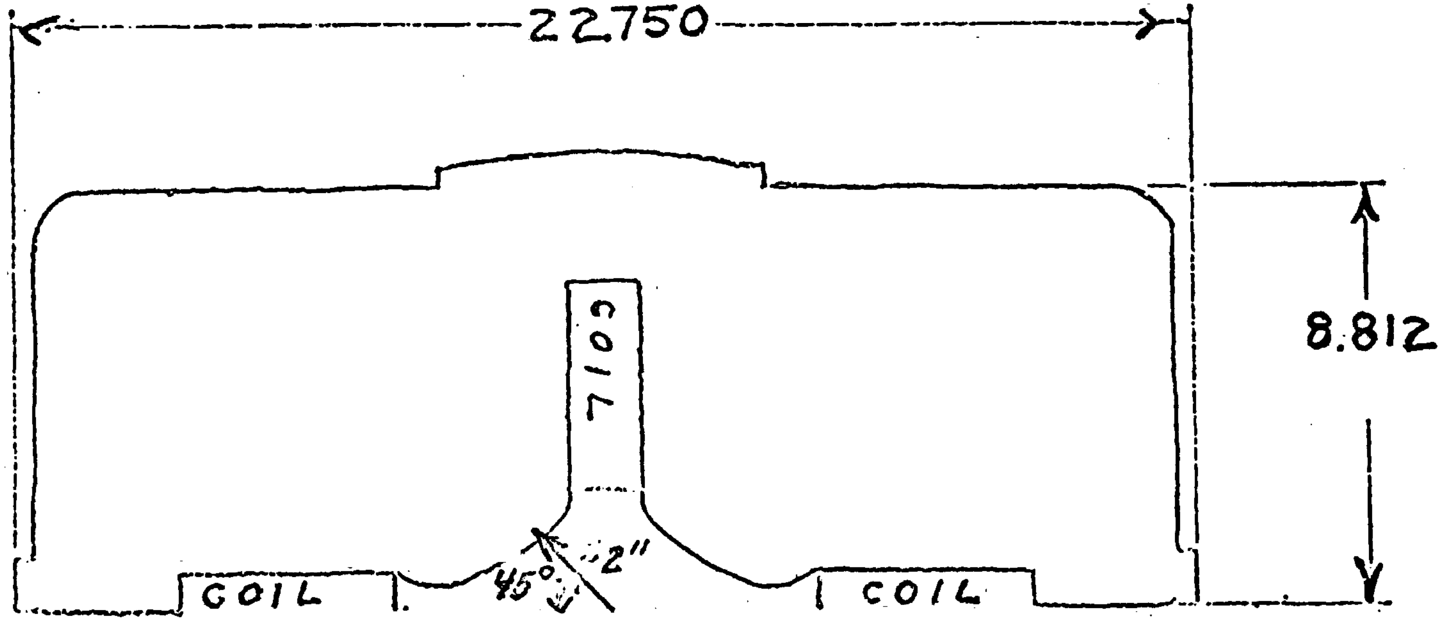

FIG. 1

QUADRUPOLE LAMINATION

ARRANGEMENT OF ELEMENTS IN TARGET BOX

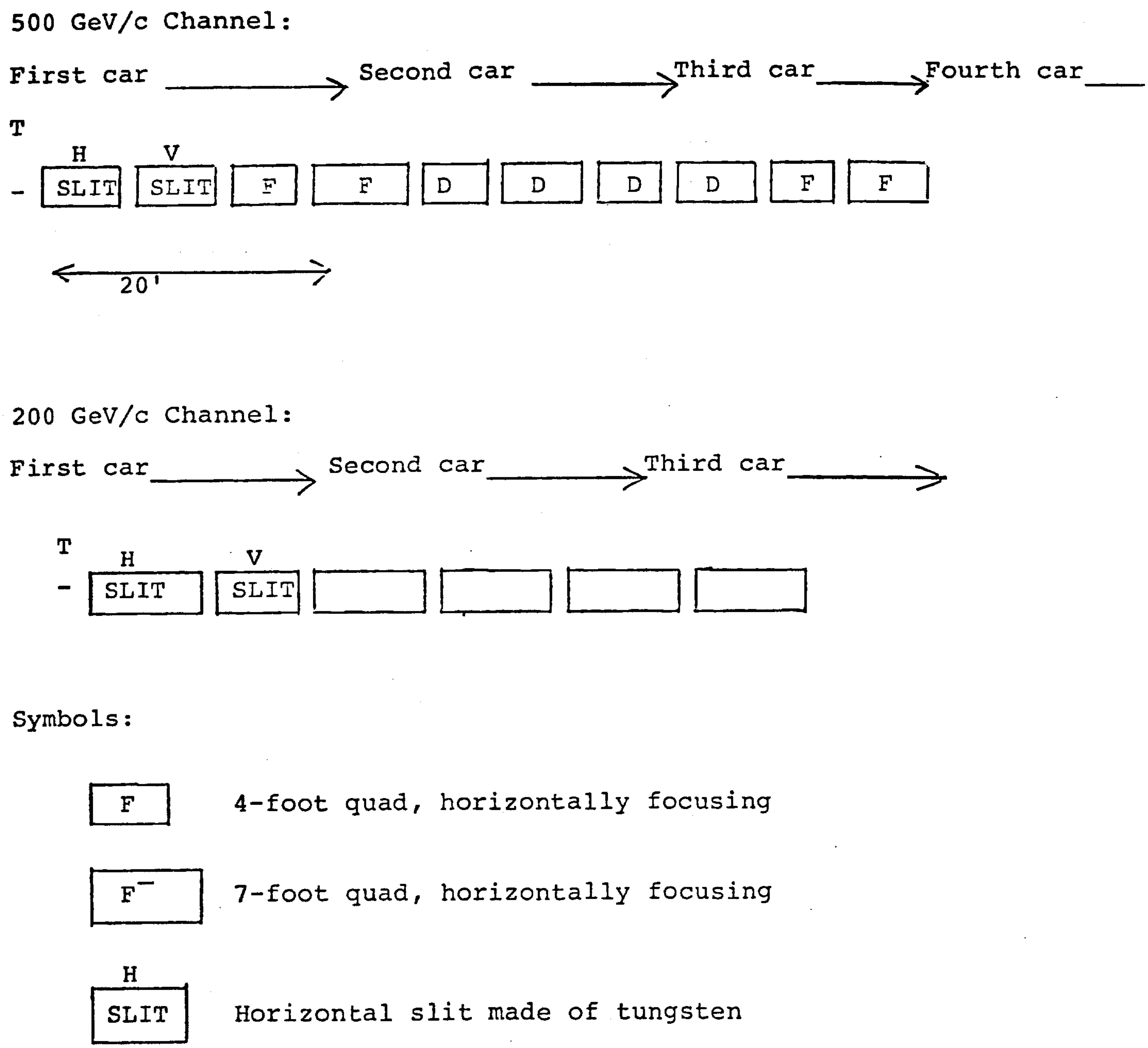

FIG. 2

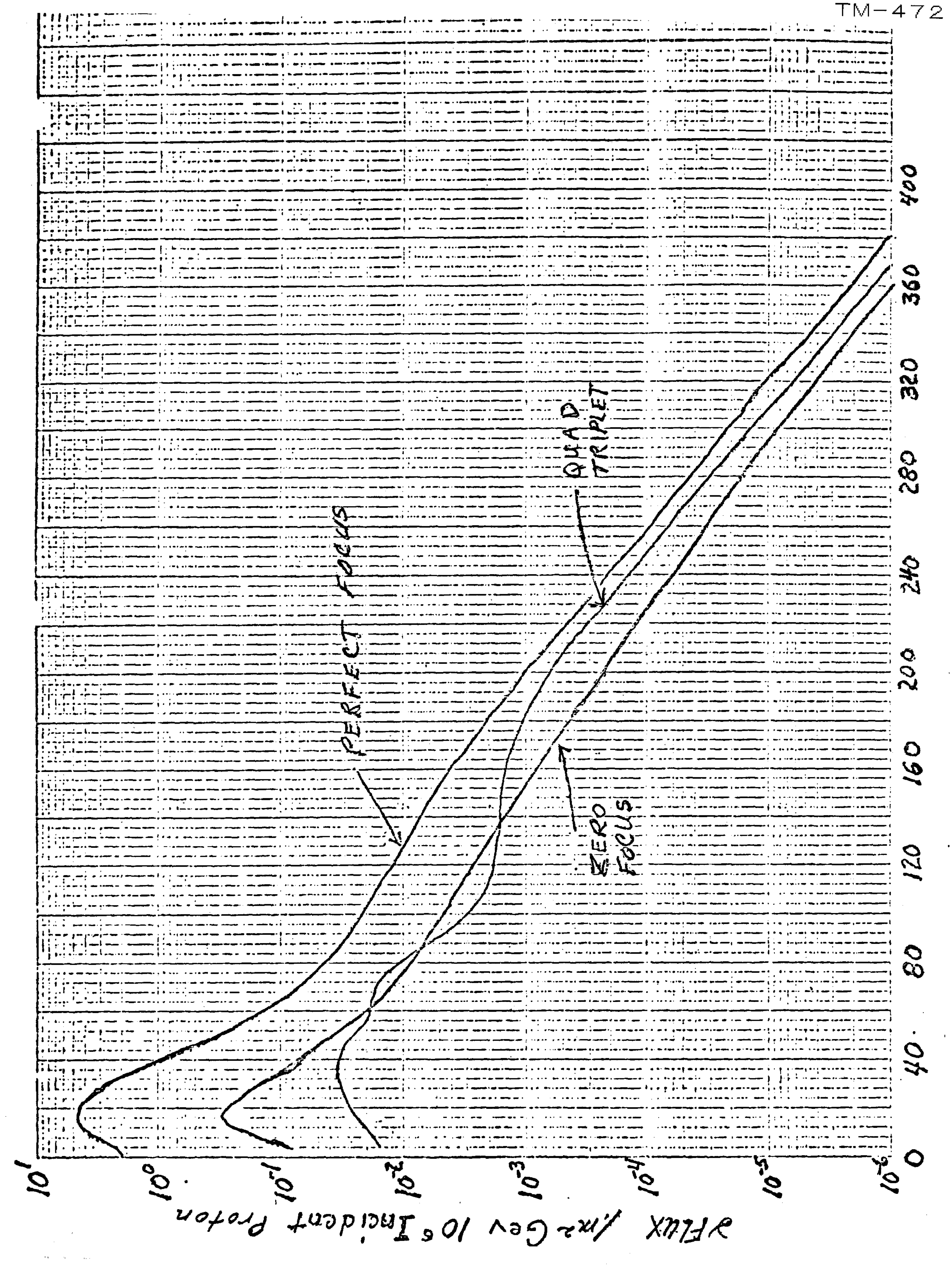
PERFECT FOCUS
QUAD TRIPLET
ZERO FOCUS
0
40
80
120
160
200
240
280
320
360
400
10^1
10^0
10^-1
10^-2
10^-3
10^-4
10^-5
10^-6
νFLUX /m² GeV 10⁶ Incident Proton

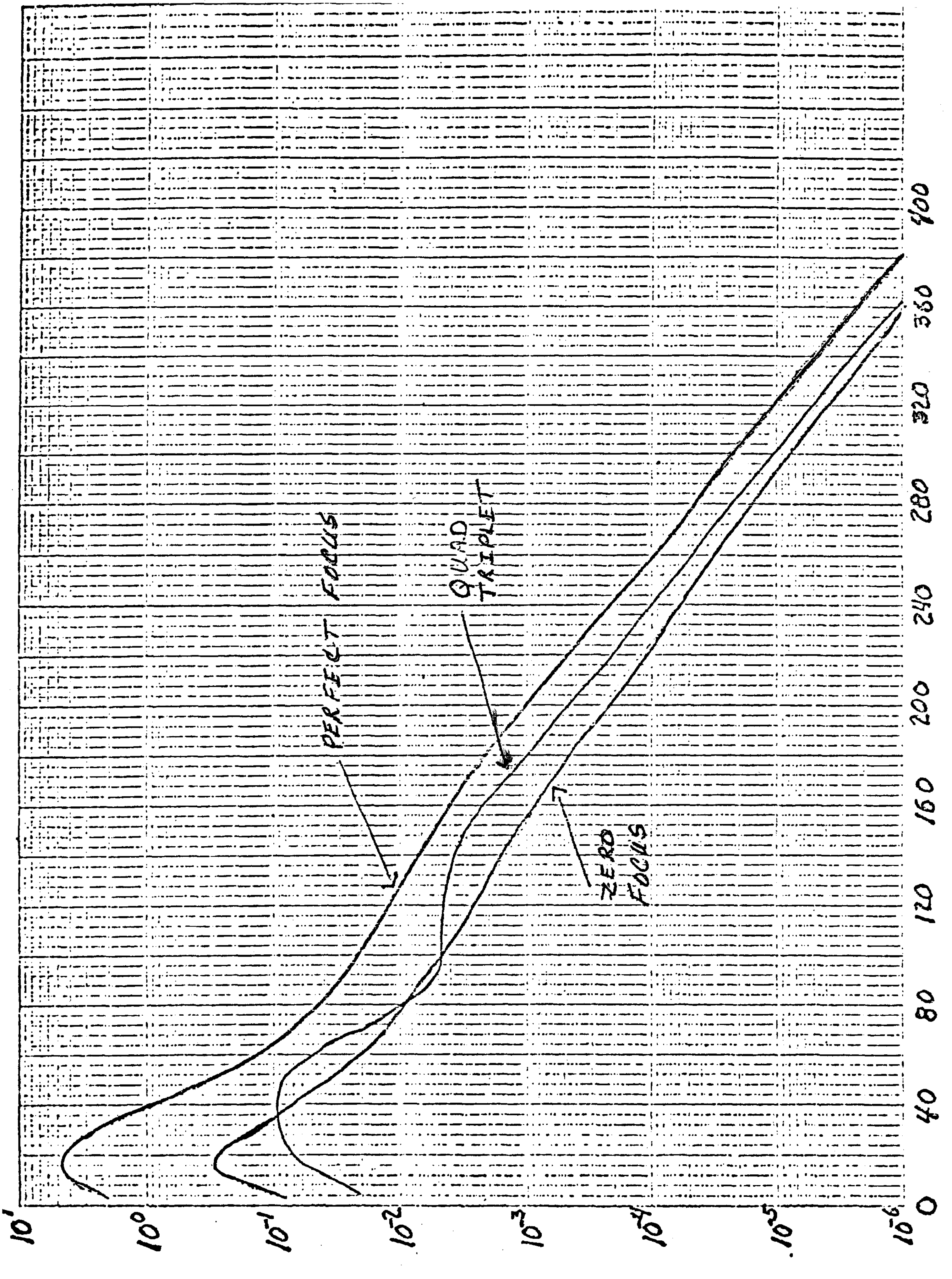
PERFECT FOCUS
QUAD TRIPLET
ZERO FOCUS
10^{1}
10^{0}
10^{-1}
10^{-2}
10^{-3}
10^{-4}
10^{-5}
10^{-6}
0
40
80
120
160
200
240
280
320
360
400
Energy — GeV

FIG. 3b.

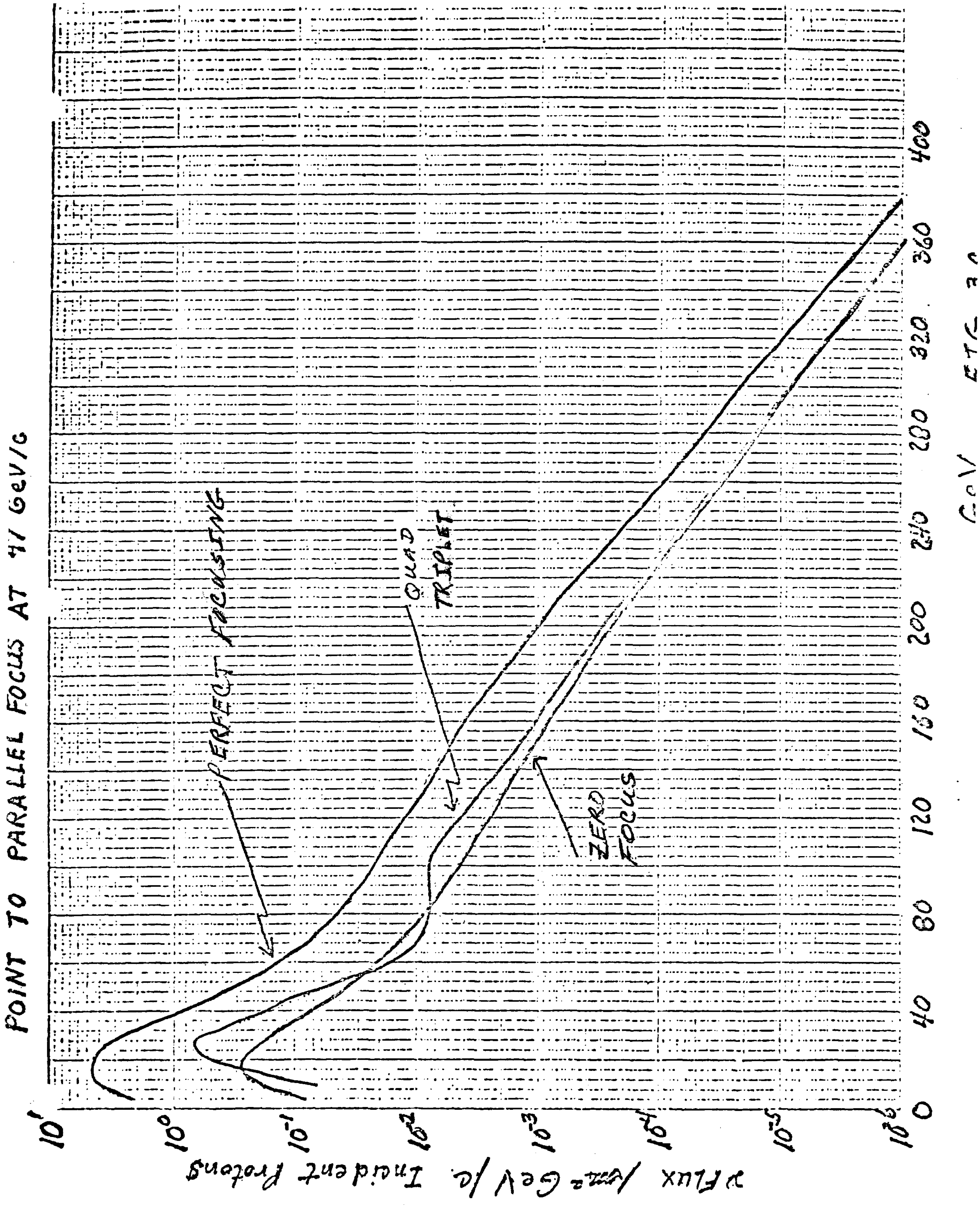
POINT TO PARALLEL FOCUS AT 47 GeV/c
PERFECT FOCUSING
QUAD TRIPLET
ZERO FOCUS
ν FLUX /cm² GeV /p. Incident Protons
GeV
0
40
80
120
160
200
240
280
320
360
400
10^{1}
10^{0}
10^{-1}
10^{-2}
10^{-3}
10^{-4}
10^{-5}
10^{-6}

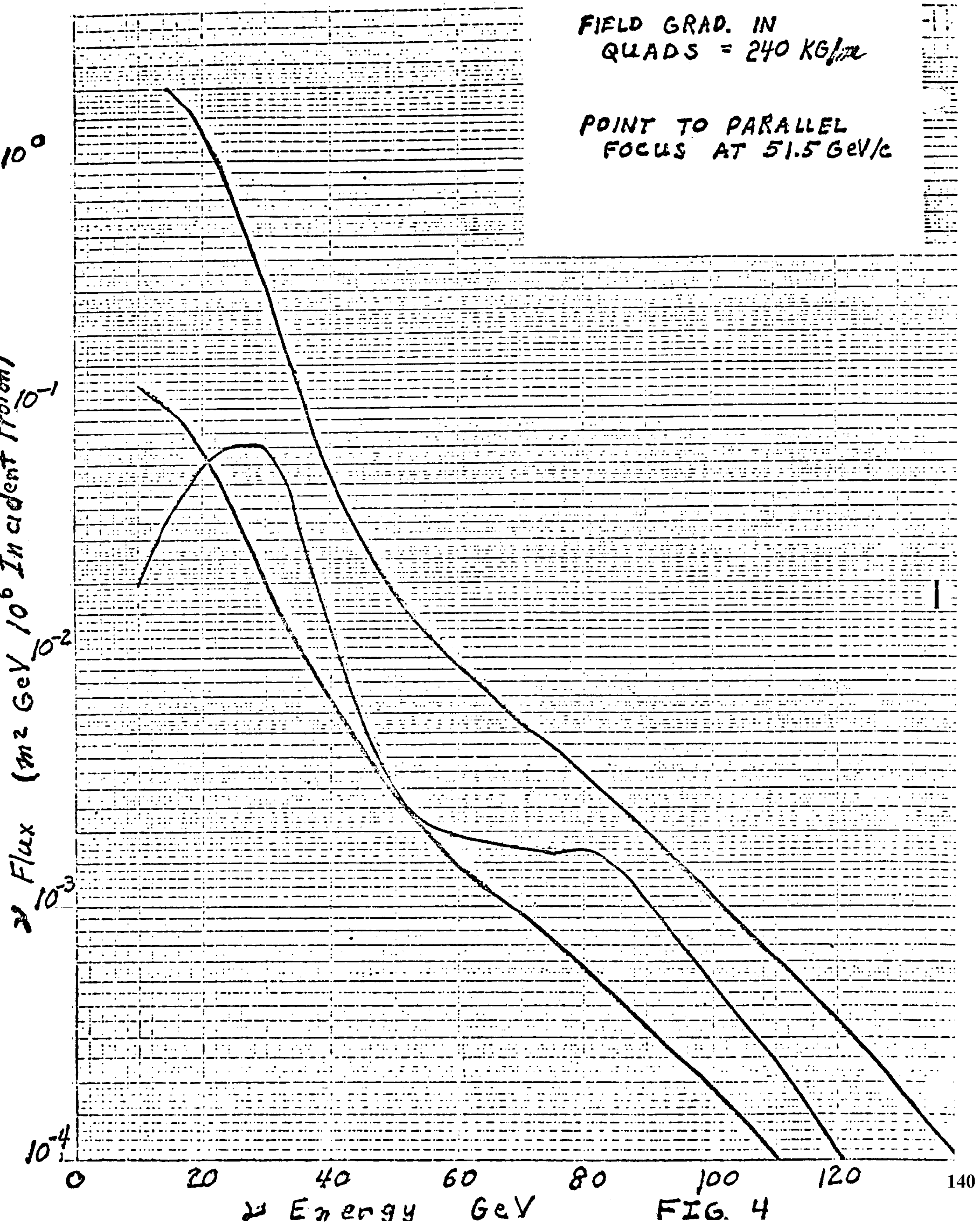
FIELD GRAD. IN QUADS = 240 KG/m
POINT TO PARALLEL FOCUS AT 51.5 GeV/c
10°
10-1
10-2
10-3
10-4
ν Flux (m² GeV 10⁶ Incident Proton)
0
20
40
60
80
100
120
140
ν Energy GeV

FIG. 4

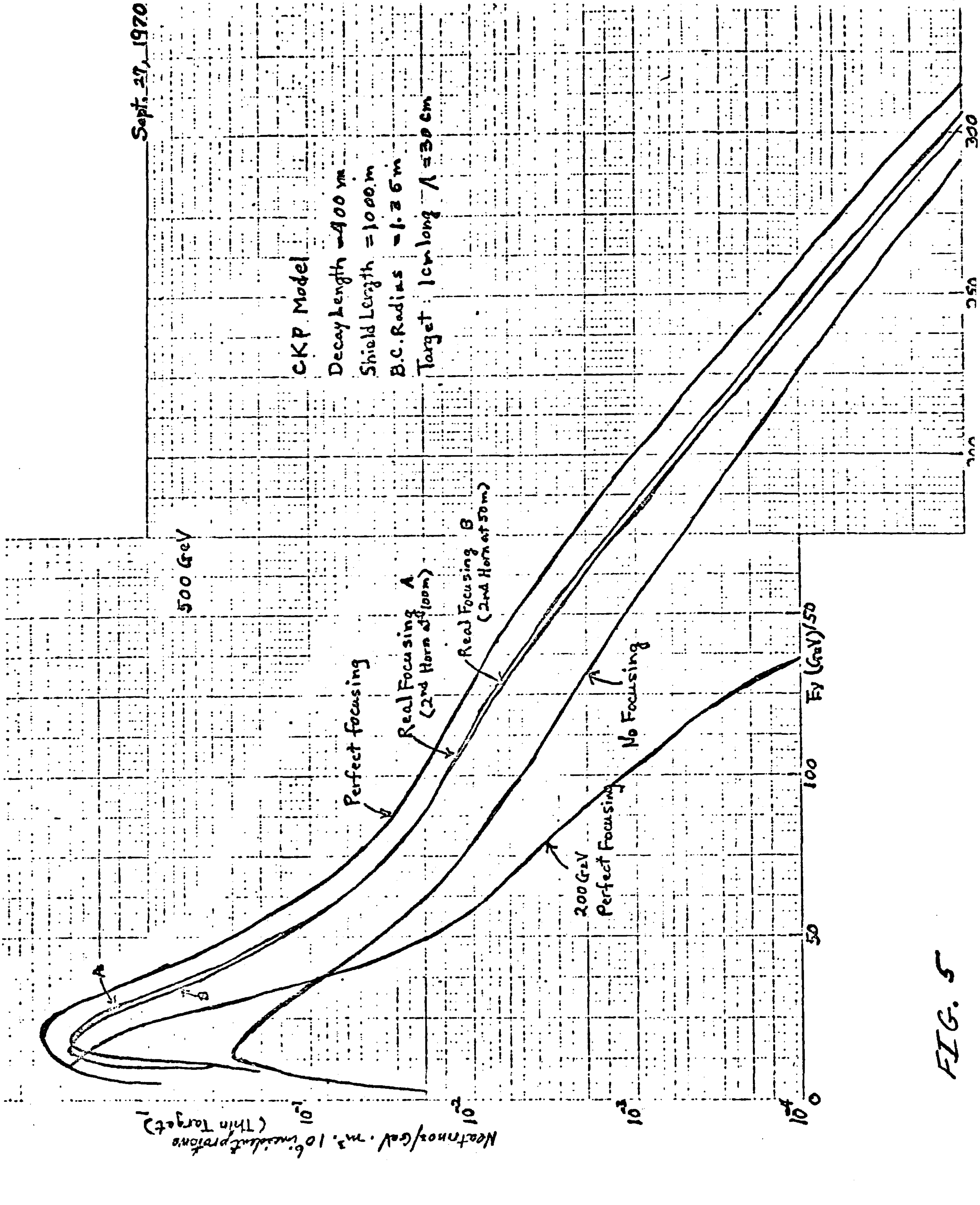
Sept. 27, 1970
CKP Model
Decay Length = 400 m
Shield Length = 1000 m
B.C. Radius = 1.25 m
Target 1cm long Λ = 30 cm
500 GeV
Perfect Focusing
Real Focusing A (2nd Horn at 100m)
Real Focusing B (2nd Horn at 50m)
No Focusing
200 GeV Perfect Focusing
A
B
0
50
100
150
200
250
300
Eν (GeV)
10^{-1}
10^{-2}
10^{-3}
10^{-4}
Neutrinos/GeV · m² · 10⁶ incident protons (Thin Target)

FIG. 5

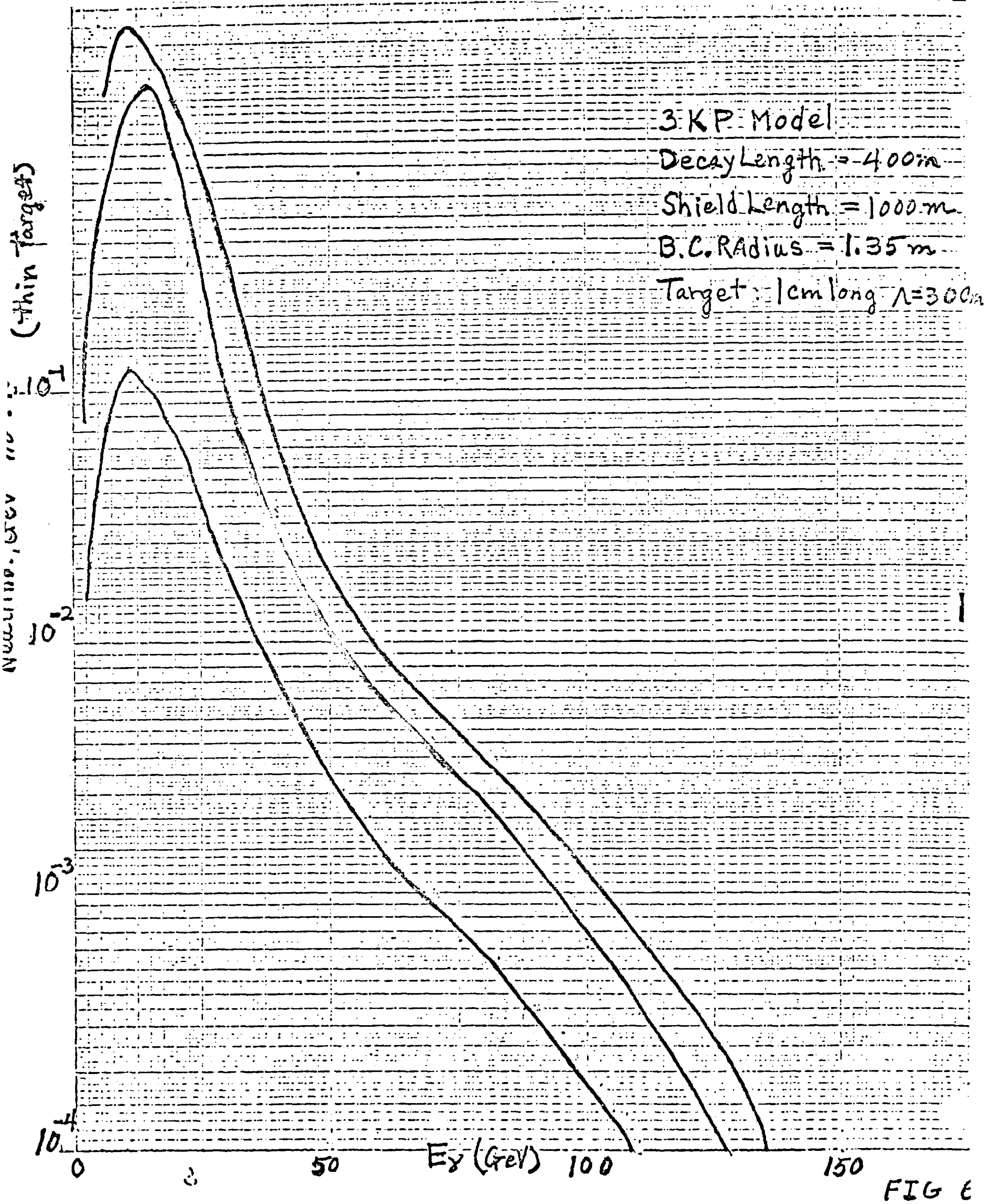
3 KP Model
Decay Length = 400m
Shield Length = 1000 m
B.C. Radius = 1.35 m
Target: 1cm long Λ=300m
(thin Target)
10⁻¹
10⁻²
10⁻³
10⁻⁴
0
50
100
150
Eγ (GeV)

FIG 6

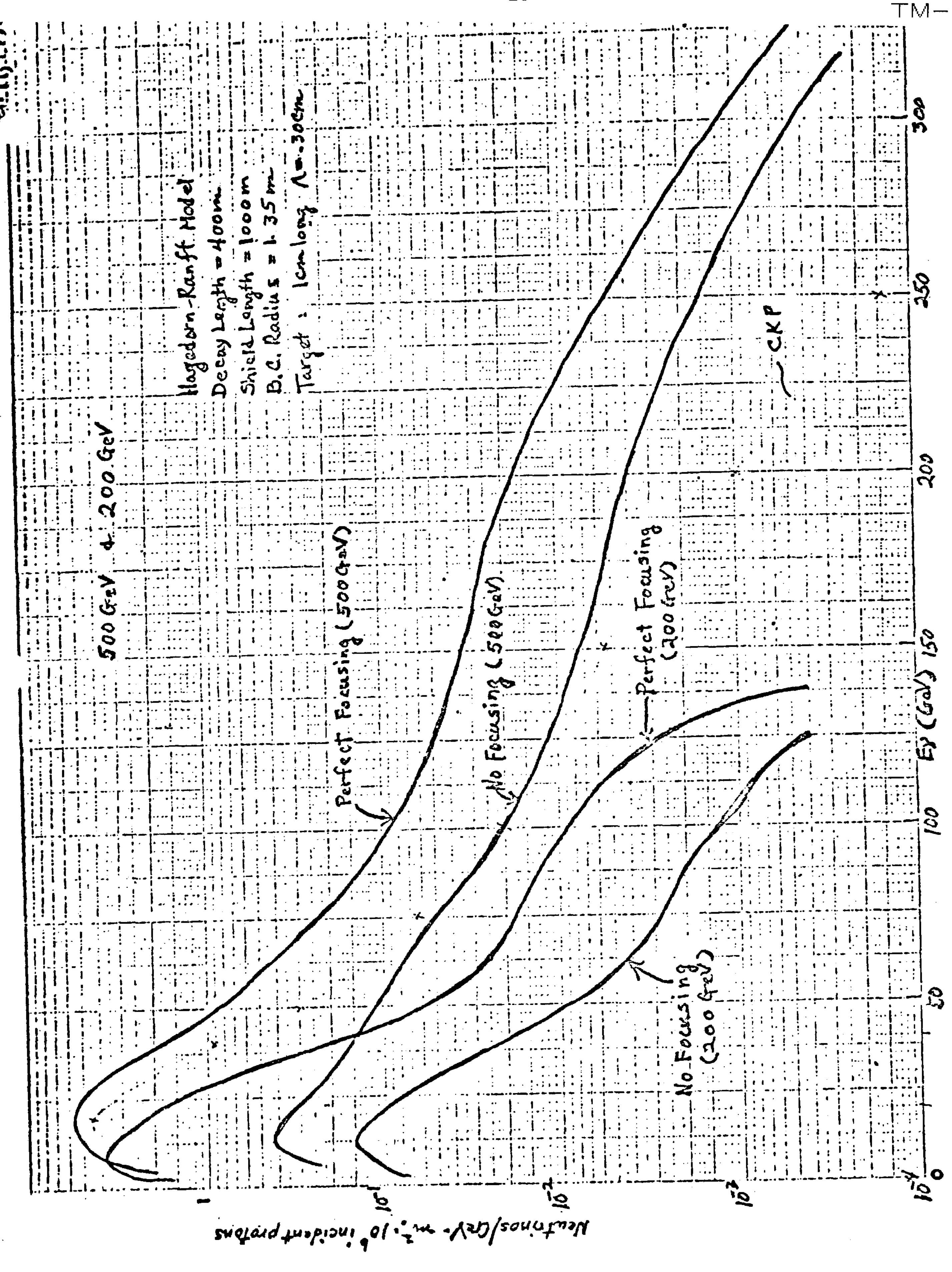
500 GeV & 200 GeV
Hagedorn-Ranft Model
Decay Length = 400m
Shield Length = 1000m
B.C. Radius = 1.35m
Target : 1cm long Λ = .30cm
Perfect Focusing (500 GeV)
No Focusing (500 GeV)
Perfect Focusing (200 GeV)
No Focusing (200 GeV)
CKP
E_ν (GeV)
0
50
100
150
200
250
300
1
10^{-1}
10^{-2}
10^{-3}
10^{-4}
Neutrinos/GeV-m^2-10^6 incident protons

Fig. 7